1.29 Synthesis of spinel-type ferrites by the Oil-in-Water microemulsion reaction method and its evaluation for photocatalytic water-splitting

Arturo A. Rodríguez Rodríguez, Miguel J. Meléndez Zaragoza, Alejandro López Ortiz, Virginia Collins Martínez, Eduardo Martínez Guerra, Margarita Sánchez Domínguez

[1] Centro de Investigación en Materiales Avanzados S. C. (CIMAV), Unidad Monterrey, Alianza Norte 202, Parque de Investigación e Innovación Tecnológica, 66600 Apodaca, México.

[2] CIMAV Unidad Chihuahua, Av. Miguel de Cervantes Saavedra 120, Complejo Industrial Chihuahua, 31136 Chihuahua, Chih. México.

* Corresponding author: tel. 8448073209, e-mail: arturo.rodriguez@cimav.edu.mx

ABSTRACT

Spinel-type ferrites have the molecular formula MFe_2O_4, where M represents a divalent metallic cation, such as Co^{2+}, Ni^{2+} and Zn^{2+} for $CoFe_2O_4$, $NiFe_2O_4$ and $ZnFe_2O_4$, respectively.As photocatalyst, spinel-type ferrites have shown an efficient visible light absorption, high sorption ability, thermal stability, and low toxicity. Moreover the magnetic response of MFe_2O_4 allows their easy recovery from the liquid reaction media. Thanks to these features, MFe_2O_4 compounds are a promising option for the photocatalytic water-splitting, a clean and simple technology to obtain H_2. In regard to the light driven production of hydrogen, the capacity of these oxides has not been fully explored, especially MFe_2O_4 nanoparticles synthesized by microemulsion. Based on this, we synthesized cobalt, niquel and zinc spinel-type ferrites employing the oil-in-water microemulsion reaction method and explored its H_2 evolution. In order to perform the photocatalytic experiments, a dispersion of nanoparticles in water (with 2% of MeOH) was prepared inside a quartz tube reactor; this system was sealed, and then illuminated with a 250 W mercurial lamp. H_2 production was monitored by gas chromatography. Prior to photocatalytic evaluation, as-synthesized nanomaterials were thermally treated and characterized. Obtained results evinced nanoparticles with a spinel-type crystalline structure and a semi-globular morphology. Furthermore, MFe_2O_4 materials exhibited an adequate surface area, visible light absorption, and a soft magnetic behavior. In the evaluation of the photoactivity, $ZnFe_2O_4$ yielded a higher amount of hydrogen (354 $\mu molH_2g^{-1}$) compared with Co and Ni ferrites in an 8 h experiment. Broadly, this work represents a novel contribution to the studies of spinel-type ferrites for the photocatalytic production of H_2.

Keywords: spinel-type ferrites; microemulsion; hydrogen production; photocatalytic water-splitting.

1.30 Review of the global delivery pathways of hydrogen fueling stations for fuel cell electric vehicles and their potential application in México

Salvador Vidal, Félix Loyola, Ulises Cano

[1]Instituto Nacional de Electricidad y Energías Limpias, Gerencia de Energías Renovables. Reforma 113, Col. Palmira, 62490, Cuernavaca, Morelos, México.

[2]Instituto de Energías Renovables. Privada Xochicalco S/N, Temixco, Morelos, México. C.P. 62580

* Corresponding author: +52 (777) 3623811 (Ext. 7140), felix.loyola@iie.org.mx

ABSTRACT

In this work, the delivery pathways of Hydrogen Fueling Stations (HFSs) for Fuel Cell Electric Vehicles (FCEVs) in the world are reviewed. The main objective is to identify the global trend or technology availability and their potential application in Mexico in the near term. The key activity is the integration of the information related with the HFSs summarized in the international government energy agencies or research centers official reports. According to the results, 372 HFSs with 36 defined delivery pathway are identified. The compressed hydrogen, off-site system, liquid hydrogen and on-site electrolysis are the more common representing 75 % of the total HFSs with a defined delivery pathway. North America prefers the compressed hydrogen delivery pathway with 40 HFSs followed by on-site electrolysis with 13 stations, and finally liquid hydrogen with 11. Europe shows almost equal delivery pathways selection between compressed hydrogen and on-site electrolysis with 33 and 30 HFSs, respectively, followed by only 8 stations with liquid hydrogen delivery pathway. On the other hand, Asia prefers off-site systems with 35 hydrogen stations along with 10 compressed hydrogen delivery pathway. At present, Japan is the country with the highest quantity of HFSs with a total of 92 active and 3 planned units. In contrast, Mexico and South American countries, with the exception of Argentina, Brazil, and Costa Rica, have none active or planned HFS for FCEVs. It is important to note that 134 HFSs detected through the sources consulted do not have a defined delivery pathway; all of them located principally in Europe and Asia. According to this, the amount of compressed hydrogen delivery pathway is higher than the on-site electrolysis followed by the offsite system and liquid hydrogen delivery. It is important to say that the compressed hydrogen, offsite system, and liquid hydrogen delivery pathways do not have a defined process for hydrogen production, but certainly it is produced in a centralized process in contrast to the on-site electrolysis pathway. On the basis of the above discussion and the natural resources available, it can be concluded that Mexico has a high potential to initiate the installation of HFSs for FCEVs using the compressed and on-site electrolysis delivery pathways supported by the emerging renewable energy market.

Keywords: Hydrogen; Delivery pathways, Hydrogen fueling stations, FCEV.

1.31 Design and integration of a hybrid electric power plant for a scooter

Carlos A. Reynoso, Iván A. Prado, Manuel de J. López, Félix Loyola, Ulises Cano

[1]Instituto Nacional de Electricidad y Energías Limpias, Gerencia de Energías Renovables. Reforma 113, Col. Palmira, 62490, Cuernavaca, Morelos, México.

* Corresponding author: +52 (777) 3623811 (Ext. 7140), felix.loyola@iie.org.mx

ABSTRACT

In this paper the design and integration of a Hybrid Power Plant (HPP) based on Proton Exchange Membrane Fuel Cells (PEMFC) for a low scale electric power traction system (scooter) is presented. The HPP consists of an in house made PEMFC stack (as the main source), a commercial battery pack and the auxiliary components that integrate the Balance of Plant (BoP), as well as the electronic control system. The BoP components include pneumatic, electronic and power electronics parts. In the control system, the electronic circuits for different functions like measurements (voltage, electrical current, PEMFC temperature, and hydrogen gas pressure), drive actuators (electro-valves and fans) and electric power conditioning were developed. The control system supervises the PEMFC general function, and it is allowed to manage the energy from PEMFC and batteries. The control system limits the PEMFC polarization to avoid stress and starvation condition. Additionally, if the electrical current demand is higher than maximum PEMFC current capacity, the batteries adds current to complete the demand. On the other hand, if the demand is lower, the PEMFC sends energy to batteries to charge it. This power source configuration and operating strategy increases the autonomy of the scooter compared with the only batteries configuration. The design proposed in this work is possible to extrapolate to a higher power traction system as an electric vehicle.

Keywords: Fuel cells; Balance of plant; Scooter.

1.32 Cu_2O/TiO_2 nanostructures for hydrogen production from methanol photoreforming

O.F. Plascencia-Hernández, G. Valverde-Aguilar, M. A. Valenzuela-Zapata

[1]Centro de Investigación en Ciencia Aplicada y Tecnología Avanzada Unidad Legaria del Instituto Politécnico Nacional,Legaria No. 694, Col. Irrigación, Delegación Miguel Hidalgo, 11500 Ciudad de México, México.

[2]Lab. Catálisis y Materiales. Escuela Superior de Ingeniería Química e Industrias Extractivas, Instituto Politécnico Nacional,Av. Instituto Politécnico Nacional No. 1936, Unidad Profesional "Adolfo López Mateos" Zacatenco C.P. 07738, Col. Lindavista, Delegación Gustavo A. Madero, 07738 Ciudad de México, México

* Corresponding author: 57296000 ext. 67763 fernandoplascenciah@gmail.com

ABSTRACT

The search of clean and energy resources is one of the main tasks in which the scientific community has paid great attention in the last decade. In such a way, the conversion of solar energy into chemical energy, especially in the formation of products such as hydrogen, hydrocarbons, alcohols, an so on, from cheap and abundant raw materials (e.g., water, carbon dioxide, glycerol, etc), is a highly desirable approach for a sustainable development. Heterogeneous photocatalysis is considered as one of the most recognized alternative to convert solar energy into useful chemicals due its the accumulated experience in environmental purification and water splitting for H_2/O_2 formation.

Photoreforming is reasonably easier than water spitting to produce hydrogen, and its use in biomass-derived substrates performing can simultaneously produce hydrogen and clean wastes. For this reason, the present investigation was focused on methanol photoreforming as viable option to pure hydrogen production.Within the wide range of photocatalysts that have been studied, TiO_2 together with Cu_2O are promising candidates for this reaction. Thus, in this work a series of Cu_2O/TiO_2 nanostructures was synthesized by chemical reduction and mixed with TiO_2 P25 at room temperature. The obtained materials were characterized by difuse reflectance spectroscopy (DRS), scanning electron microscopy (SEM) and X-ray photoelectron spectroscopy (XPS). According to our results, Cu_2O spheres with an average size of 180 nm were homogeneously dispersed on TiO_2 and the best hydrogen production rate was obtained with a 0.06:1 Cu_2O:TiO_2 molar ratio after 8 h of irradiation using simulated solar light. An explanation for this surprising behavior was made in terms of a weak interaction between the two oxides.

Keywords: Cu_2O/TiO_2; hydrogen; methanol photoreforming

1. Introduction

In the last decade, heterogeneous photocatalysis has shown great advances in aspects related to the environment and energy, among others [1]. For instance, the efficient hydrogen production from water splitting in the presence of a suitable semiconductor and sunlight is emerging as an attractive option to solve simultaneously real problems to the impending energy crisis and environment pollution [2]. However, the task is not easy, there must be a material capable of performing a coupled strong water oxidation and reduction, besides of showing a high stability and low cost. Tiatanium dioxide (TiO_2, n-type semiconductor) has been the most studied material for this reaction, although due to the high value of its band gap (E_g= 3.2 eV) demands UV-light for its activation, which is only available in 3-4% in the whole radiant solar energy [3,4]. On the other hand, another of the disadvantages of TiO_2 is its fast recombination of photogenerated electron–hole pairs, during hydrogen evolution reaction [5].

For this reason, several options have been conserted to improve the photocatalytic activity of TiO_2 under visible light, among which it can be mentioned: (i) surface modification via organic materials, (ii) band gap modification by nonmetals, (iii) metals doping and (iv) semiconductor coupling [6]. Particularly, combining a n-type semiconductor with a p-type semiconductor (e.g. Cu_2O), to form a heterojunction, is an efficient method to separate the photoinduced electrons and holes due to the effect of the inner electric field [7]. Cu_2O with a direct-band of 2.0 eV, with virtual non-toxicity and natural abundance, has been widely explored by several research groups on applications for water splitting, solar cell, gas sensor, and so on [8]. Furthermore, the Cu_2O/TiO_2 system has been studied showing promising photocatalytic results in many reactions [7,8], which has been explained in terms of an enhanced charge separation due to the photogenerated electrons from Cu_2O conduction band can transfer to the conduction band of TiO_2, and the holes can migrated from valence band of TiO_2 to the valence band of Cu_2O.

The goal of this research was to synthesize Cu_2O/TiO_2 nanostructures at room temperature in two steps. In the first stage, Cu_2O uniform polyhedra were obtained by chemical reduction process; after that, TiO_2 P25 was added over the Cu_2O polyhedra, controlling the ethanol/water relationship. Under this procedure, it was synthesized four materials, varying the Cu_2O/TiO_2 molar ratio. Difuse reflectance spectroscopy (DRS), scanning electron microscopy (SEM) and X-ray photoelectron spectroscopy were the main characterization techniques employed. The photocatalytic activity of the prepared materials was tested in the methanol photoreforming reaction using a solar simulator as the radiation source.

2. Materials and Methods

2.1 Materials

Copper (II) chloride ($CuCl_2$; 97%), sodium hydroxide (NaOH; 98.2%), L-ascorbic acid (99.5%), Polivinilpilorridone (PVP; M_W 55,000), titanium dioxide P25 Degussa (TiO_2 P25; 99.5%) were purchased from Aldrich and used without further purification. Aqueous solutions were prepared using deionized water (Milli-Q with 18.6 MΩ) and ethanol reagent grade (denatured).

2.2 Synthesis of Cu_2O polyhedral

Cu_2O polyhedral particles were synthesized at room temperature by the chemical reduction route. Sodium hydroxide solution (1M, 40 mL) was prepared and stirred vigorously and then, a copper chloride solution (0.15 M, 40 mL) was added drop by drop and stirred for 15 minutes. After that, a 60 mL of PVP:L-ascorbic acid solution (1.42 weight ratio) was added fast and the final solution was stirred for 30 minutes. The resultant Cu_2O polyhedral particles were washed three times with a 1:1 water:ethanol solution, and dry under air atmosphere for storage.

2.3 Synthesis of Cu_2O/TiO_2 composite

Cu_2O polyhedral particles were dissolved in a water:ethanol (1.25 volume ratio) solution. At the same time, titanium dioxide P25 was dissolved in a water:ethanol solution (1.5 volume ratio) an added to a 100 mL Cu_2O solution and stirred for 30 minutes. Following the same procedure, four composites with a molar ratio (Cu_2O:TiO_2): A=0.6:1, B=0.3:1, C=0.06:1 and D=0.03:1, were synthesized.

2.4 Characterization

UV–vis diffuse reflectance spectra (DRS) were obtained in a GBC Cintra 20 spectrometer on the range of 200-800 nm. Scanning electron microscopy (SEM) analysis was carried out on a JEOL 7800F microscope. XPS analyses were performed using a ThermoFisher Scientific K-Alpha X-ray photoelectron spectrometer with a monochromatized AlKα X-ray source (1487 eV).

2.5 Photocatalytic evaluation

The Cu_2O/TiO_2 composites were evaluated in hydrogen production by means of methanol photoreforming. An Hg-Xe lamp (200 W) was used as irradiation source without any type

of filter. Initially, it was prepared a methanol:water solution (1:5 volume ratio) and the photocatalyst was dissolved maintaining a concentration of 1 mg/mL. The resulted solution was stirred in the dark for 30 min to perform the adsorption process. After that, the reactor was placed in front to the light source, and irradiated for 8 h. The gas effluent from the reactor was analyzed every hour by gas chromatography.Cu_2O polyhedral particles and TiO_2 P25 were also evaluated separately at the same reaction conditions.

3. Results and Discussion

3.1 Scanning electron microscopy

Figure 1a) shows Cu_2O polyhedral particles with average size of 196 nm. The facets of the structure clearly are appreciated, but is not possible determine exactly their number. Some agglomeration zones can be observed. The commercial TiO_2 P25 is presented Fig.1b), without a clear shape or structure, only agglomerates of nanoparticles. Figures 1c) to 1f) correspond to the Cu_2O/TiO_2 composites. The identification of the Cu_2O polyhedral particles is more difficult when the molar ratio decreases. Composite A (0.6:1) is showed in Fig. 1c). The Cu_2O polyhedral particles are close to P25 nanoparticles, probably by an electrostatic interaction. Figure 1d) shows composite B (0.3:1), where the Cu_2O polyhedral particles are more surrounded by P25 particles and still it is possible to identify them. The composite C (0.06:1) and D (0.03:1) are showed in Figures 1e) and 1f). Cu_2O polyhedral particles were not identified, only P25 nanoparticles, because the molar ratio was very low.

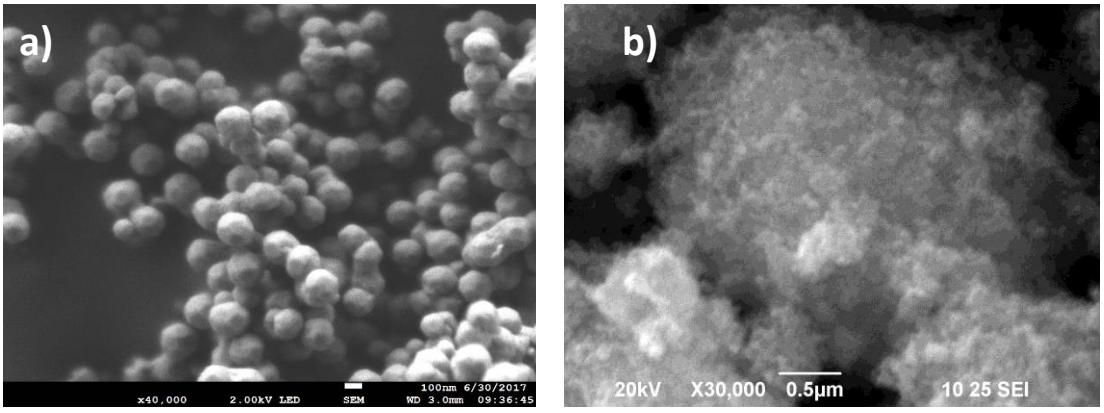

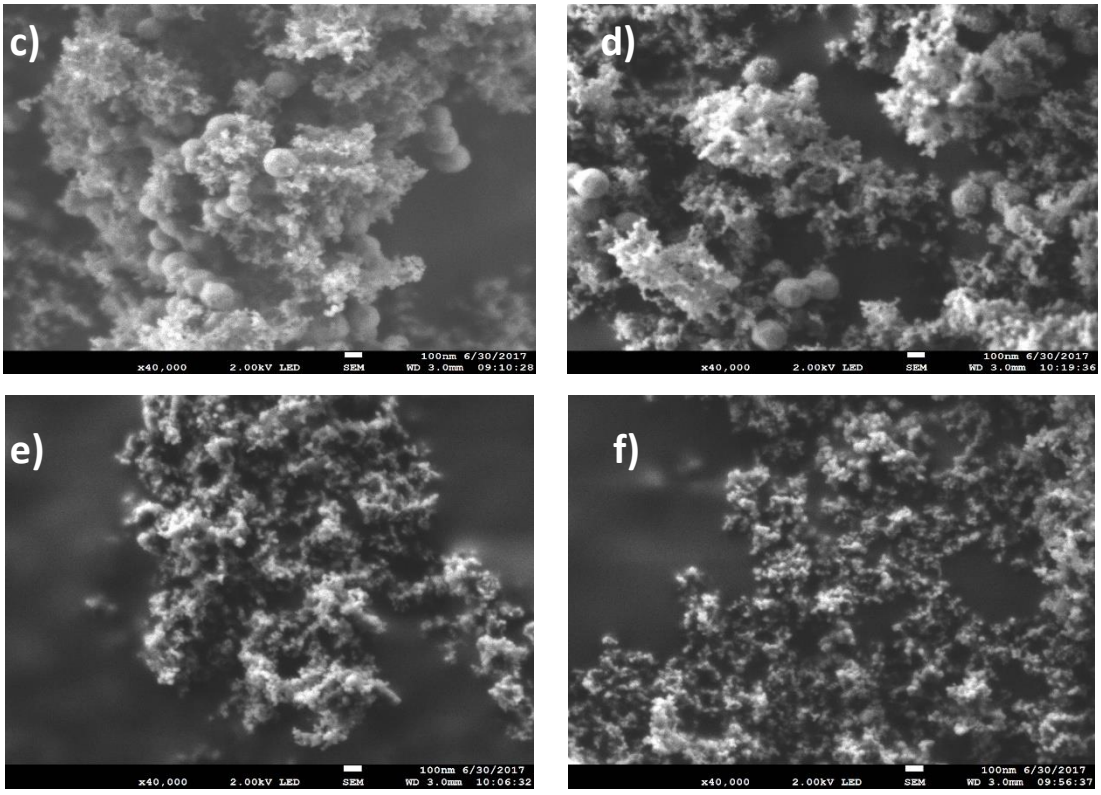

Fig. 1. SEM analyses of synthesized structures ofa) Cu_2O polyhedral particles, b) commercial TiO_2 P25, composites (Cu_2O/TiO_2): c) A (0.6:1), d) B (0.3:1), e) C (0.06:1), f) D (0.03:1)

3.2 Diffuse Reflectance Spectroscopy

Absorption spectra of the Cu_2O polyhedral particles, P25 and Cu_2O/TiO_2 composites are presented in Fig. 2a). As can be seen, the Cu_2O particles showed a clear photon absorption in the visible range and P25 only in the UV region. The Cu_2O/TiO_2 composites presented two strong adsorption peaks on the visible and UV regions that was interpreted as separate contribution of each compound to the global spectrum shown in Fig. 2a). Figure 2b) shows a plot of hv vs $(\alpha hv)^2$ and the band gap energy of Cu_2O polyhedral particles were determined as an average value of 2.18 eV, and for commercial P25 was 3.3 eV, which were similar to those reported in the literature [4].

a) **b)**

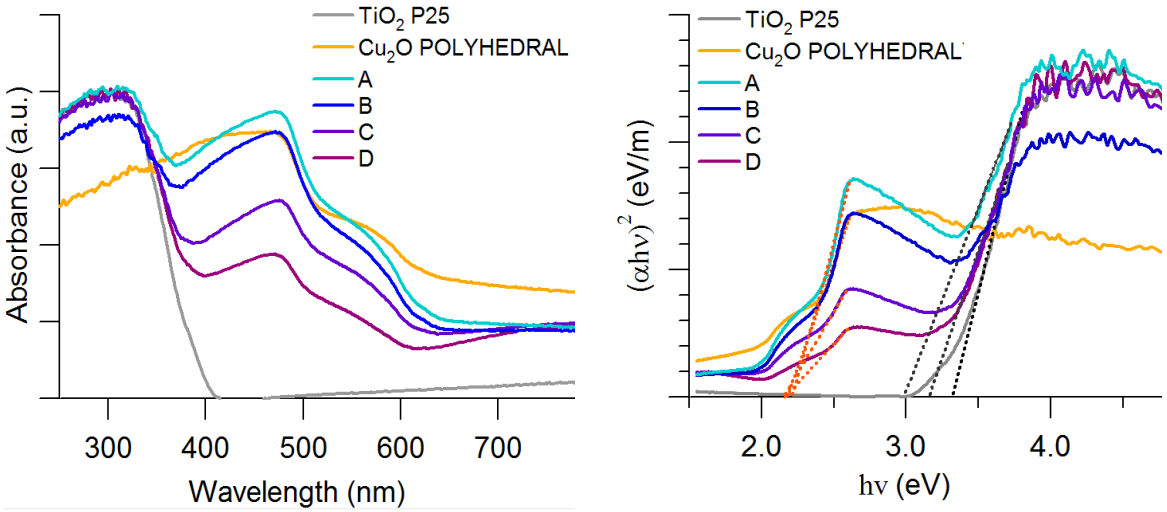

Fig. 2. a) Absorption spectra of composites, Cu_2O polyhedra and the commercial P25, b) Plot of hv vs $(\alpha hv)^2$

3.3 XPS

XPS spectra of photocatalyst C, fresh and spent after 8 h irradiation time are shown in Fig.3. Cupprous oxide characteristic peaks at 932.48 eV and 952.28 eV binding energies correspond to Cu2p3/2 and Cu2p1/2 of cuprous oxide,Fig 3a. After irradiation, a slight decrease in the signals of Cu_2O was detected. Figure 3b) shows two peaks at 458.28 eV and 464.08 eV, correspond to Ti2p3/2 and Ti2p 1/2, respectively. Finally, one peak was at 529.58 eV corresponding to oxygen 1s was localizated.These results revealed the presence of cuprous oxide species which showed photocatalytic stability after 8 h of irradiation time without any interaction with TiO_2. It seems that both oxides were mixed but each one maintaining their original properties.

3.3 Photocatalytic activity

The results for hydrogen production by methanol photoreforming are shown in Fig. 3. Cu_2O polyhedral particles did not show photocatalytic activity under the reaction conditions. The commercial P25 has a slightly hydrogen production. All Cu_2O/TiO_2 composites showed a higher photocatalytic activity than that presented by each oxide separately. The maximum hydrogen production was reached by the composites C and D, with the less molar ratio of Cu_2O polyhedral particles, with a value around 136 μmol/gr.

a) **b)**

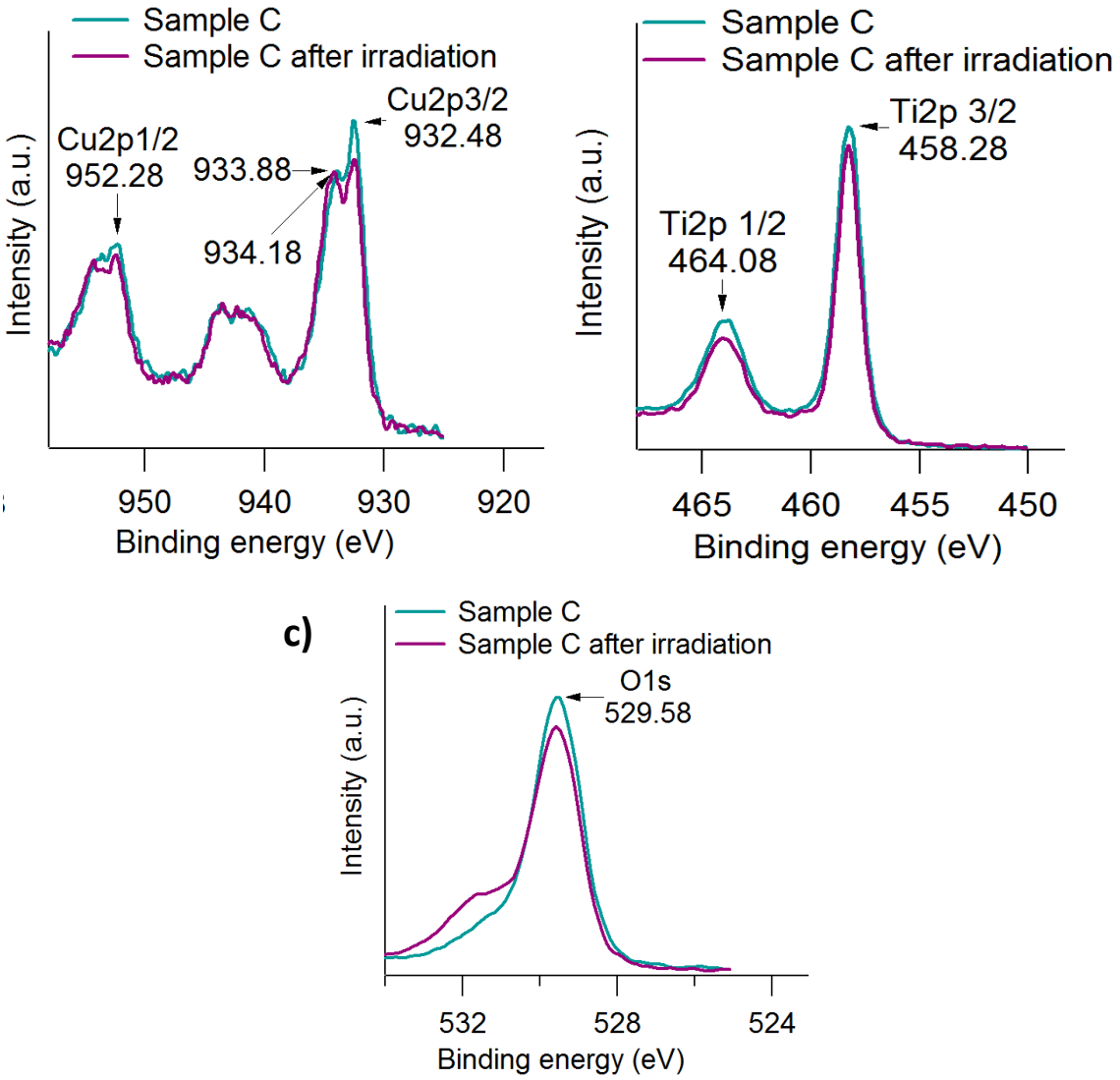

Fig. 3. a) Peaks of copper b) Peaks of titanium,c) Peaks of oxygen d) New peaks after irradiation

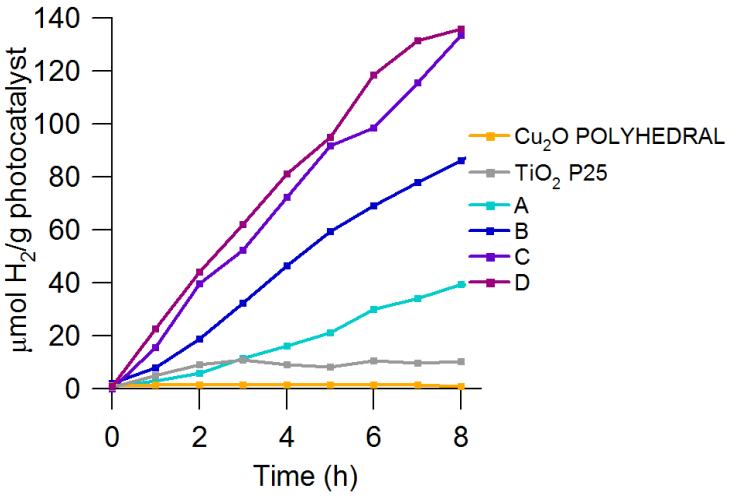

Fig. 4. Hydrogen production by methanol photoreforming under solar simulator.

4. Conclusion

Cu_2O polyhedral particles were synthesized successfully at room temperature.The Cu_2O/TiO_2 composites conserved their specific band structure with a minimal interaction. The closeness of the two oxides was enough for improving the charge separation in the photocatalytic system and the highest hydrogen production compared to each oxide.

Acknowledgements

The authors acknowledge the financial supports of SIP 20170002 and SIP 20171127. FPH is grateful for CONACyT and BEIFI fellowships.

References

[1] Li Y, Wang B, Liu S, Duan X, Hu Z. Synthesis and characterization of Cu2O/TiO2 photocatalysts for H2 evolution from aqueous solution with different scavengers. Appl Surf Sci 2015;324:736–44. doi:10.1016/j.apsusc.2014.11.027.

[2] Rahman MM. H2 production from aqueous-phase reforming of glycerol over Cu-Ni bimetallic catalysts supported on carbon nanotubes. Int J Hydrogen Energy 2015;40:14833–44. doi:10.1016/j.ijhydene.2015.09.015.

[3] Jung M, Hart JN, Boensch D, Scott J, Ng YH, Amal R. Hydrogen evolution via glycerol photoreforming over Cu-Pt nanoalloys on TiO2. Appl Catal A Gen

2016;518:221–30. doi:10.1016/j.apcata.2015.10.040.

[4] Huang L, Peng F, Wang H, Yu H, Li Z. Preparation and characterization of Cu2O/TiO2 nano-nano heterostructure photocatalysts. Catal Commun 2009;10:1839–43. doi:10.1016/j.catcom.2009.06.011.

[5] Han T, Zhou D, Wang H, Zheng X. The study on preparation and photocatalytic activities of Cu2O/TiO2 nanoparticles. J Environ Chem Eng 2015;3:2453–62. doi:10.1016/j.jece.2015.09.020.

[6] Falah M, MacKenzie KJD. Synthesis and properties of novel photoactive composites of P25 titanium dioxide and copper (I) oxide with inorganic polymers. Ceram Int 2015;41:13702–8. doi:10.1016/j.ceramint.2015.07.198.

[7] Liu L, Yang W, Sun W, Li Q, Shang JK. Creation of Cu2O@TiO2 composite photocatalysts with p - N heterojunctions formed on exposed Cu2O facets, their energy band alignment study, and their enhanced photocatalytic activity under illumination with visible light. ACS Appl Mater Interfaces 2015;7:1465–76. doi:10.1021/am505861c.

[8] Geng Z, Zhang Y, Yuan X, Huo M, Zhao Y, Lu Y, et al. Incorporation of Cu2O nanocrystals into TiO2 photonic crystal for enhanced UV–visible light driven photocatalysis. J Alloys Compd 2015;644:734–41. doi:10.1016/j.jallcom.2015.05.075.